

## **Binder Jetting of High Temperature and Thermally Conductive (Aluminum Nitride) Ceramic**

**Carlos A. Diaz-Moreno<sup>1\*</sup>, C. Rodarte<sup>1</sup>, S. Ambriz<sup>1</sup>, D. Bermudez<sup>1</sup>, D. Roberson<sup>1</sup>, C. Terrazas<sup>1</sup>, D. Espalin<sup>1</sup>, R. Ferguson<sup>2</sup>, E. Shafirovich<sup>2</sup>, Y. Lin<sup>1</sup> and Ryan B. Wicker<sup>1</sup>**

<sup>1</sup>W. M. Keck Center for 3D Innovation. College of Engineering E-108. University of Texas at El Paso.  
University Ave. 500 W, El Paso TX. 79968, USA.

<sup>2</sup>Department of Mechanical Engineering, The University of Texas at El Paso.

\*Corresponding author:

**[cdiazmoreno@utep.edu](mailto:cdiazmoreno@utep.edu)**

**Keywords:** Ceramics; Aluminum nitride; 3D components fabrication; Thermal conductivity; Binder jetting; Additive manufacturing;

### **Abstract**

This work reports on the novel fabrication of aluminum nitride (AlN) complex components using binder jetting, on the use of sintering and hot isostatic pressing (HIPing) to increase their density, and on the characterization of the printed material, including thermal conductivity. The HIPing parameters employed were a temperature of 1900 °C using a rich nitrogen atmosphere at a pressure of 30,000 psi during 8 h. Results show that the printed and HIPed AlN components had a 1.96 g/cm<sup>3</sup> (60.12%) density when compared to theoretical values. The thermal conductivity for densified and HIPed components was measured in the range from 23 °C to 500 °C resulting in values from 4.82 W/m\*K to 3.17 W/m\*K, respectively. Characterization using scanning electron microscopy, energy dispersive X-ray spectroscopy and X-ray diffraction was used to investigate the ceramic structural morphology of the sintered and HIPed material, its chemical composition, and crystal structure of the binder jetting manufactured AlN components.

### **1. Introduction**

#### **1.1 Introduction to Additive Manufacturing**

Additive manufacturing (AM) is a novel 3D fabrication process for a wide range of materials, such as polymers, metals and ceramics [1]. The fabrication by AM refers to processes in which material is added in layers guided by computer aided design (CAD) model to create a three-dimensional object [2]. There are distinct AM technologies including vat-photopolymerization, material extrusion, and binder jetting (BJ), just to mention few [3]. In the last decade, there has been an increasing effort to characterize AM ceramic materials by using different techniques [3-5], namely with diverse spectroscopic techniques such as X-ray diffraction (XRD) spectroscopic and electron optical and surface chemical characterization techniques. The recent advances in small-scaled electronics, combined with computational equipment had allowed scanning electron microscopy (SEM) to see morphology and chemical analysis through energy dispersive X-ray spectroscopy (EDS) in specific areas of samples under investigation to study the surface of fabricated components [2].

## **1.2 Introduction to BJ process**

The BJ process is a suitable technique for fabrication of 3D structures from precursor ceramic powder materials. The BJ process uses two main materials; a powder material and a binder. The binder acts as an adhesive between the powder layers and it is dispensed selectively into the powder bed through an inkjet print head that is able to displace along the "X" and "Y" axes of the machine. After printing, the binder can be cured, and a de-binding step carried out using the appropriate thermal post-processing [2]. Several steps are incurred in BJ processing of ceramic components: first, the ceramic powder material is spread over the build platform using a roller; second, the inkjet print head deposits the binder as adhesive on top of the powder where required by the design of the component; and third the build platform is lowered by a prescribed layer thickness, and another layer of ceramic powder is spread over the previous layer. Steps 1 through 3 are repeated until the entire component has been printed. A schematic of the BJ process is shown in Figure 1.

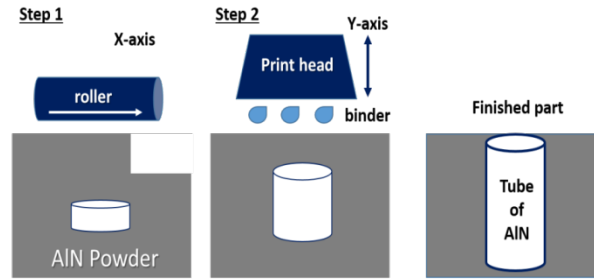


Figure 1. Schematic representation of BJ process

### 1.3 AlN ceramic material

AlN has been used in the electronic industry since the past decade due to its combination of remarkable properties, such as wide band gap, high thermal conductivity, low thermal expansion, high strength, optical transparency, and piezoelectric properties [4]. AlN is a covalently bonded ceramic, it is synthesized from aluminum ( $^{13}\text{Al}$ ) and nitrogen ( $^{14}\text{N}$ ) in the stoichiometric as presented in Table 1. It does not occur naturally, and once synthesized it is stable in inert atmospheres at temperatures over 2100 °C. After fabrication of ceramic materials, components are sintered and also subjected to hot isostatic pressing (HIPing) method to improve densification. The HIPing method requires high pressures and temperatures intervals at different cycles under inert atmosphere [5]. The ability to use BJ for the fabrication of AlN exhibiting high thermal conductivity and strong dielectric properties, highlights the potential for the fabrication of components or devices for future electronic packaging applications [3].

Table 1. AlN stoichiometric chemical composition

Element	Symbol	At. mass (g/mol)	# of atoms	% of mass
Aluminum	Al	26.9815	1	65.8275 %
Nitrogen	N	14.0067	1	34.1725 %

In this work, we report on the characterization of the thermal and other material properties for AlN produced using BJ, and highly densified through the use of post-fabrication heat treatments, for the first time. The components were fabricated using an ExOne M-lab equipment. After fabrication, components were sintered and also subjected to HIPing method to improve densification. After sintering and HIPing, various properties of the material, including thermal

conductivity, crystal structure and chemical composition, were analyzed using SEM, EDS, and XRD.

## 2. Experimental Details

### 2.1 Fabrication of components by BJ

In this work, the AlN precursor powder was sourced from American Element, with a measured purity of 99.9%. The powder had an average particle size of  $\sim 45 \mu\text{m}$ . Fabrication of components was performed in an ExOne M-Lab (Irwin, PA serial number: 0600H2). Other fabrication parameters used included a binder saturation level of 200%, powder packing ratio of 57.62%, and a feed ratio to layer of 1.75. Several geometries were designed and fabricated to test the resolution capabilities of the BJ to process AlN. The geometries included a set of tubes having a diameter of 1", and varying thicknesses of 1/8", 1/16", 1/32", and 1/64"; at two different heights of 1" in and 1/2", respectively. Other geometries built included pellets with a diameter of 1/2" and thickness of 0.11". The flow diagram for BJ of AlN components fabrication process is shown in Figure 2. The flow diagram shows the followed BJ fabrication process which main stages go under fabrication, densification and characterization of material properties.

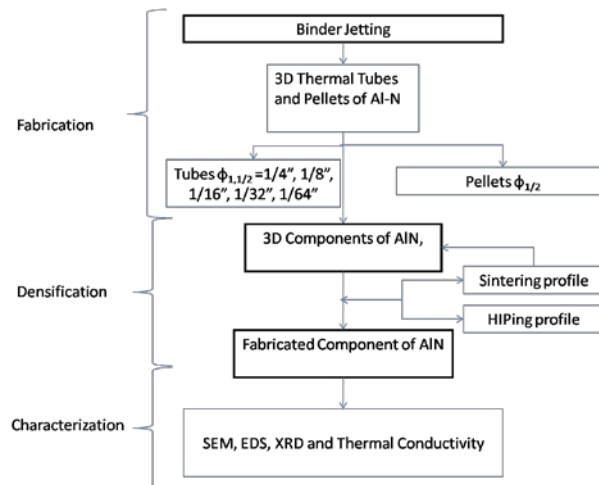


Figure 2. Fabrication flow diagram process for BJ of AlN components

#### 2.1.1 Curing, sintering and HIPing parameters

After printing, the AlN green bodies were subjected to a binder curing thermal process at 200 °C for 2 h. After curing, a sintering cycle was performed in a Sentro Tech furnace 1600. A first sintering cycle was performed, at 1500 °C for 1h with and without vacuum conditions and without use of a carbon crucible in order to understand the densification and chemical composition of fabricated components inside the furnace elements. . A second sintering cycle was performed with vacuum and in an inert atmosphere and using a carbon crucible. Then, the furnace was vacuum purged three times at -27 inHg, and a positive flow of argon (Ar) was used to create an inert atmosphere. Then, the sintering cycle was set with a ramp rate of 5 °C/min, followed by three dwell ramps at 150 °C for 1 h, 600 °C for 20 min and at 1500 °C for 5 h. The three dwell ramps used achieved humidity removal, binder evaporation, and increased the strength of AlN components, respectively. Finally, using an AIP-30H furnace model, a HIPing cycle was tested to increase the density of the fabricated components. The HIPing cycle consisted of a ramp rate of 5°C/min at 1900 °C in a nitrogen atmosphere at 30,000 psi with an 8 h hold. The sintering and HIPing profile used are presented in figure 3.

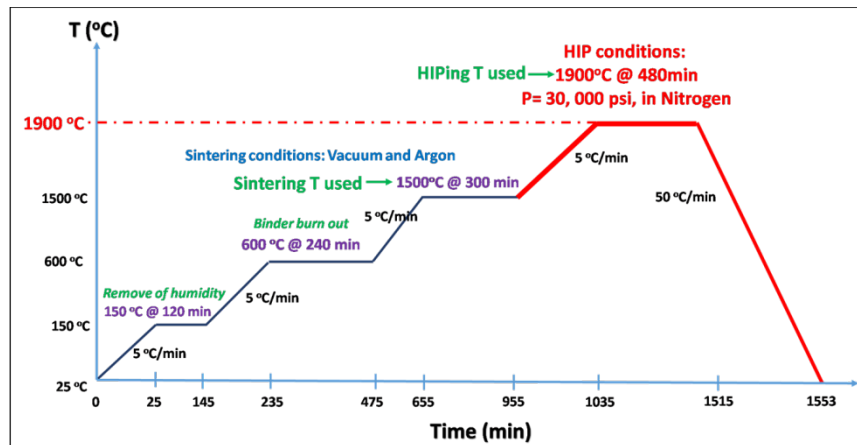


Figure 3. Sintering and HIPing parameters used to densify AlN components.

### 2.1.2 Shrinkage and density measurements

The dimensional shrinkage analysis (DSA) was done using a Metrology Multisensor OGP with a zoom up for accuracy of 10x magnification. The DSA of fabricated components with sintering and HIPing required the measurements of components at exterior diameter ( $D_{ext}$ ), interior diameter ( $D_{int}$ ), and wall thickness (width), respectively. Density measurements of manufactured

components were calculated using the standard density formula where the mass is divided by its volume.

## **2.2 SEM and EDS**

Morphology aspects and chemical analysis were performed by using a SEM from HITACHI SU3500 system with an integrated EDS spectroscopy from OXFORD Instrument X-Max<sup>N</sup> brand, respectively.

## **2.3 XRD**

XRD was done using a PANalytical Empyrean system with a CuK $\alpha$  radiation source at 40 keV and 30 mA in the  $2\theta$  range between 20° and 80°, at 0.02° steps every 4 seconds. The AlN crystallographic indexation was done using #ICDD: 00-025-1133 for hexagonal (C<sub>6v</sub><sup>4</sup>-P6<sub>3</sub>mc).

## **2.4 Thermal conductivity measurements**

The thermal conductivity (TC) measurements were performed using a Netzsch LFA 457 MicroFlash table-top instrument that uses the laser flash method (LFM) for thermal diffusivity measurements. The LFM is capable of determining the specific heat profile by using graphite or any standard that is pre-loaded into the software. Because the software knows what to expect from the graphite standard, it has a reference point for comparison to determine the specific heat of the unknown sample. Two pellet components of AlN with a diameter of 0.5” and thickness of 0.11” were employed for this experimental at sintering and HIPing parameters, respectively.

## **3. Results and Discussion**

### **3.1 Fabrication of components by BJ**

The ExOne M-Lab was used to successfully produce various components out of AlN precursor powders. Tubes with the dimensions previously discussed were all successfully fabricated. No

particular issues were found for any of the produced components, even those that were tall and had the smallest thickness. Figure 4 shows the BJ produced green body AlN tube with a 1" diameter, thickness of 1/64", and height of 1", after curing at a temperature of 200 °C for 2 h.

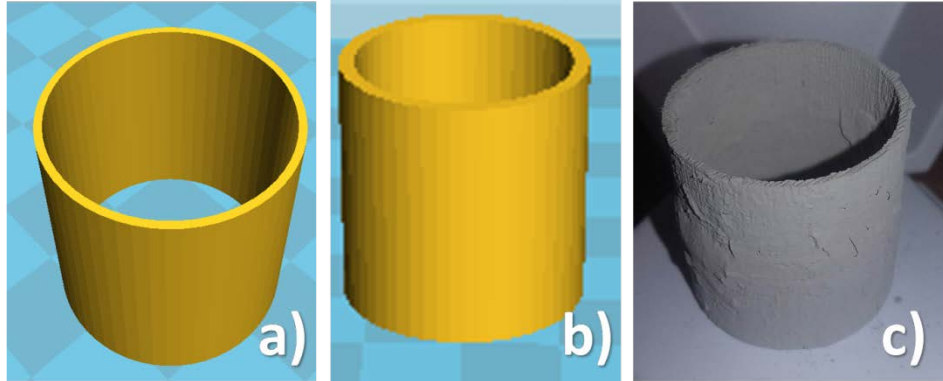


Figure 4. Tube different views; a) and b) CAD design of tube with a 1" diameter, thickness of 1/64", and height of 1"; c) Printed green body AlN tube after curing at 200 °C for 2 h.

The fabrication of this component required 18h and 35 min, consisting of 260 deposited layers of AlN powder (at a layer thickness of 45 $\mu$ m), a spread powder layer time of 20 mm/sec and using 22 passes of binder in between layers. It is worth mentioning that the AlN phase is easy to lose during fabrication and sintering of components due to the covalent bond between Al and N easy to contaminate at temperatures between 1500 °C to 1850 °C [6, 7]. Figure 5a) shows the tube after the sintering thermal process under vacuum conditions. As it can be appreciated, the tube maintains its grey color, which indicates that is related to the AlN phase. Figure 5b) shows the tube without vacuum conditions (open atmosphere). During sintering in an open atmosphere, a color change can be observed, where the material turned from grey to white which is related to a potential nitradation (oxidation) that occurred during the sintering process without vacuum thermal conditions.

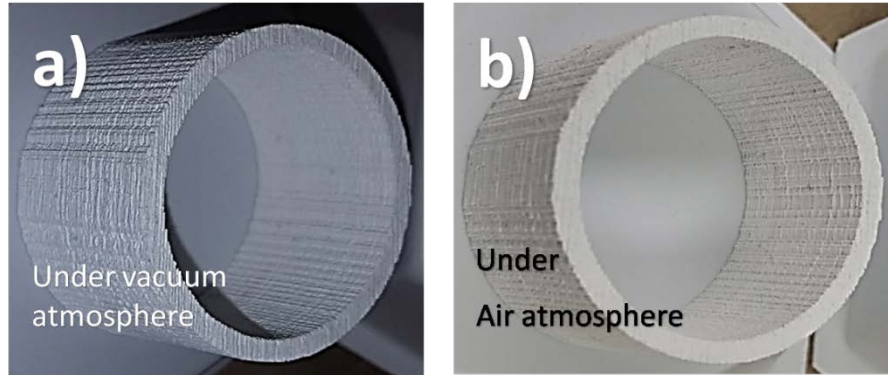


Figure 5. a) AlN tube component sintered under vacuum conditions; b) AlN tube sintered in air conditions turned into aluminum oxide ( $\text{Al}_2\text{O}_3$ ).

Furthermore, Figure 6a) shows the tube after the sintering thermal process for de-binding (brown body). As it can be appreciated, the tube turned to a black color, which was attributed to the use of a glassy carbon crucible to protect the AlN tube from potential oxidation or contamination from the furnace heating elements during the sintering process.

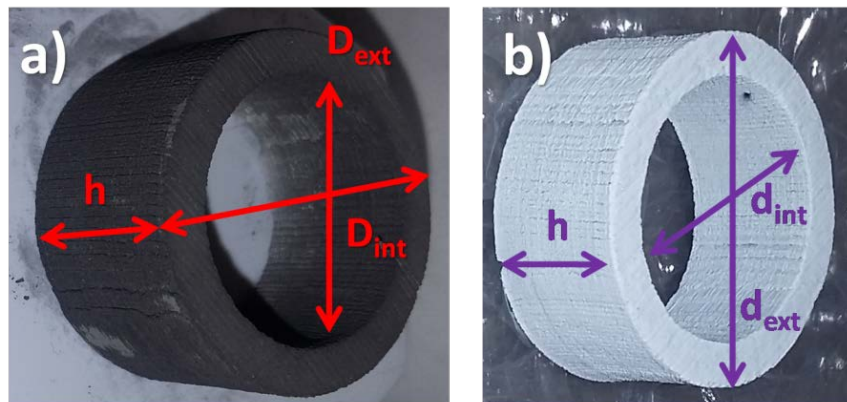


Figure 6. a) Tube after the sintering thermal process using a carbon crucible to avoid oxidation and b) tube after HIPing process showing the white-grayish related to AlN composition.

Finally, the finished AlN tube was subjected to the HIPing cycle to increase its densification. Figure 6b) shows the tube after the HIPing cycle. The tube changed coloration from black (sintered tube sample) to white-grayish which is related to AlN ceramic phase [7]. It is worth mentioning that components were produced using BJ without sintering aids.

### 3.1.1 Shrinkage and density measurements

The 1” diameter, 1/8” thickness tube component was measured using a SmartScope OGP to calculate the shrinkage it experienced after the post-processing steps of sintering and HIPing. Figure 7 shows the image as seen from the SmartScopeOGP top view of a segment of HIPed tube. It shows good packaging of the layers, a good texture and well defined and uniform edges around the surface of the component.

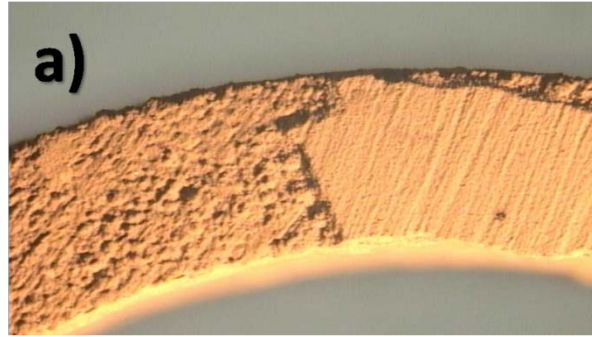


Figure 7. a) Picture of a segment at top view of AlN tube after HIPing process.

Table 2 shows the calculated shrinkage experienced by the AlN tube with nominal external diameter and wall thickness of 1”and 1/8”, respectively. Compared with the nominal values in the as fabricated condition, specimens that were sintered and subjected to the HIPing cycle had overall shrinkage values of: -0.025”, -0.001” and +0.111” for the external, internal diameters and wall thickness dimensions (width).

Table 2. Tube with sintering and HIPing for dimensions analysis.

<b>Tube</b>	<b>D<sub>ext</sub>(in)</b>	<b>D<sub>int</sub>(in)</b>	<b>Width(in)</b>
<b>With sintering</b>	<b>0.994</b>	<b>0.731</b>	<b>0.003</b>
<b>After HIP</b>	<b>0.968</b>	<b>0.730</b>	<b>0.115</b>
<b>(with sintering - after HIP)</b>	<b>-0.025</b>	<b>-0.001</b>	<b>+0.111</b>

The measurements taken with the SmartScopeOGP showed that there was shrinkage of dimensions of the AlN 3D printed components which are in a complete agreement with HIPing process for sintering ceramics materials [6-8]. The reported density measured for this AlN tube at various stages during the fabrication ranged from ~ 1.07 g/cm<sup>3</sup> after curing at 200 °C, ~ 1.13 g/cm<sup>3</sup> after sintering at 1500 °C, and finally to ~ 1.96 g/cm<sup>3</sup> after the HIPing cycle. The density

values mentioned correspond to ~ 32 %, ~ 35 %, and ~ 60 % of the theoretical density for AlN [7].

### 3.2 SEM-EDS

Microscopy through SEM was employed to characterize the density of components. One of the reasons densification is difficult, is because of trapped gases evolved from the powder surface or the decomposition of binder trapped in closed pores [8]. It is well known that the post thermal processing for AlN is difficult to achieve due to its covalent nature [9].

#### 3.2.1 Sintering with and without vacuum conditions

The fabricated components were analyzed by SEM and EDS, the first analysis was performed with samples that were subjected to sintering process conditions with and without vacuum at 1500 °C and no without use of a carbon crucible, were studied to understand the thermal behavior of the material in different thermal conditions at the same temperature.

Figure 8a) shows a representative SEM image at 2000X magnification from the AlN component sintered at 1500 °C with vacuum and without crucible protection. Figure 8b) shows the EDS corresponding to the chemical analysis found in sintered component. The percent content of chemical elements found were 38%, 60% and 12%, for aluminum, oxygen and molybdenum respectively. The traces of molybdenum (Mo) were attributed to contamination coming from the furnace heating elements made having a chemical composition containing this element. It is worth mentioning that besides oxygen, AlN has a high affinity for Mo which induces contamination [7].

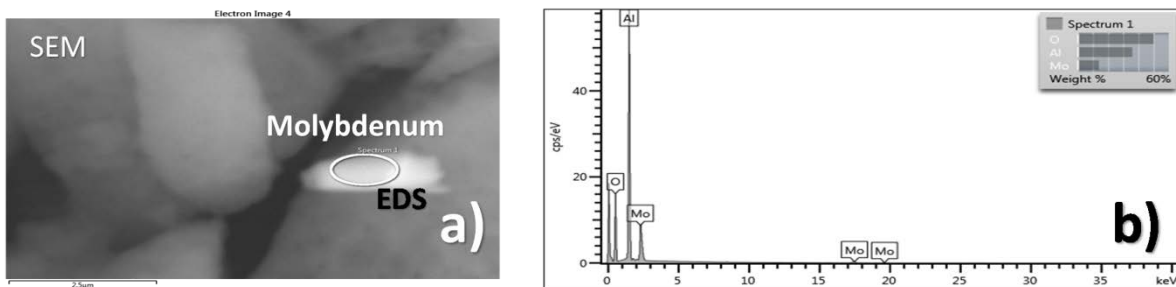


Figure 8. AlN sintering at 1500 °C at vacuum without crucible; a) SEM and b) EDS

Figure 9a) shows the SEM image of the component sintered at 1500 °C without vacuum and no crucible covering. The image shows random sized AlN polycrystals joined together without sintered particles properties. Figure 9b) shows the corresponding EDS (from the area indicated in Figure 8a). In the image, it can be seen that chemical elements Al, O and Fe were found at 52%, 47% and 3% content respectively. This confirmed that the components would have undergone oxidation. Figure 9c) and 9d) show EDS maps showing profiles in green aluminum and red for oxygen.

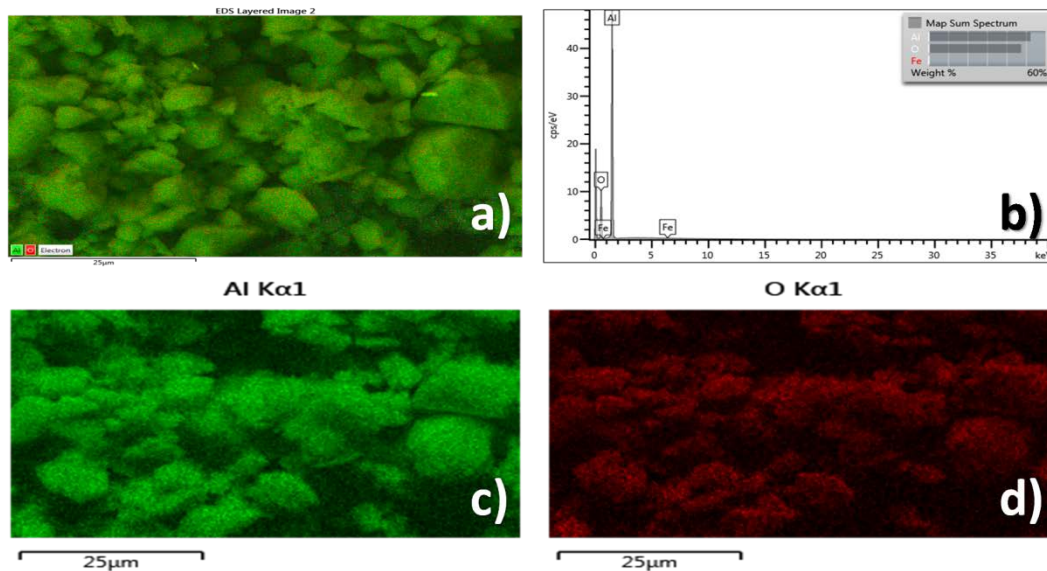


Figure 9. AlN sintering at 1500 °C in air atmosphere.

EDS results for both sintered samples with and without the use of vacuum and no crucible covering, showed that contamination was present in components as exhibited by the presence of Mo and Fe, which were related to the sintering furnace heating elements. As mentioned before oxygen is well known combining to AlN, it was observed a potential presence of oxygen within the components with and without vacuum of 60% and 47%, respectively.

### 3.2.2 Sintering under Ar atmosphere and HIPing

Furthermore, sintering conditions were explored using the vacuum and argon (Ar) inert atmosphere and with a carbon crucible to protect components from furnace chamber

contamination. Figure 10 from a) to d) shows a set of SEM images at different magnifications of the morphology structure profile of the component subjected to a sintering thermal treatment at 1500°C in Ar atmosphere and vacuum conditions. This image indicates agglomerations of particles and cluster of smaller microparticles bound together due to the binder, the compaction created by the roller during printing, and the sintering conditions.

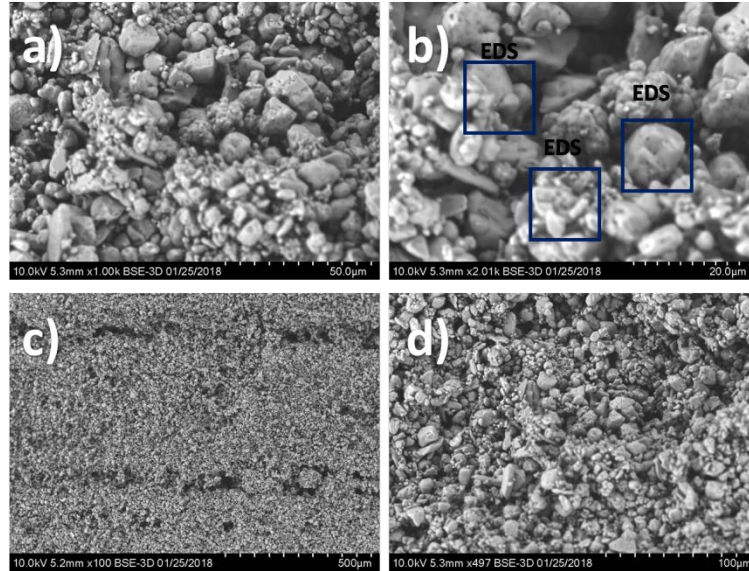


Figure 10. From a) to d) SEM images of AlN at different magnifications with sintering at 1500 °C in Ar atmosphere/vacuum and covering with a carbon crucible.

The regions indicated in blue squares in Figure 10b) correspond to the regions that were used for EDS chemical analysis composition. The EDS results were found to consist of 65% Al, 15% N, and 15% C, respectively. The occurrence of carbon was traced to the use of a glassy carbon crucible in order to protect the components being sintered from the heating elements. The crucible and inert gas atmosphere aided in preventing metallic contamination traces from the interior of the furnace and avoid oxidation of material.

Figure 11a) shows a representative SEM image at the cross section of the AlN tube that was subjected to the HIPing process at 1900 °C. This view allows observation of homogeneous sintered microparticles exhibiting coalescence with well-formed boundaries. The regions indicated in white squares were used for EDS chemical analysis composition results.

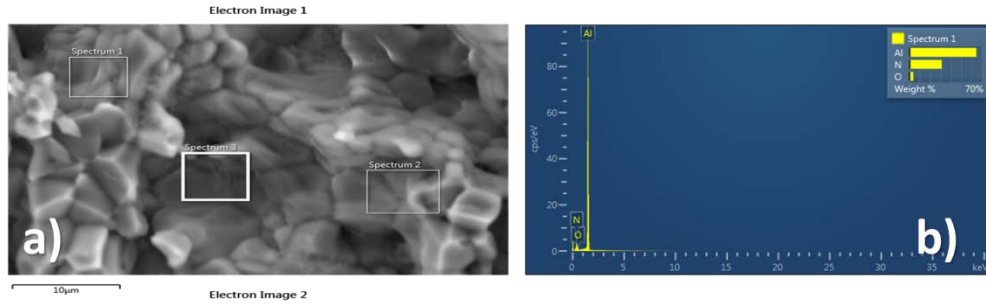


Figure 11. a) SEM of AlN with HIPing cycle at 1900 °C and b) EDS results.

Figure 11b) corresponds to the EDS results, showing that the components subjected to the HIPing cycle had a chemical trace corresponding to 65% Al, 32% N, and 3% O. This chemical composition obtained belongs to original atomic/mass of Al and N in AlN stoichiometric composition. The oxygen trace can be the result of trapped porous structures due to the fabrication process.

### 3.3 XRD

The formation of pure crystalline AlN phase by HIPing cycle was confirmed by XRD. Figure 12 shows the XRD results of AlN printed components after the HIPing process at 1900 °C. The XRD pattern for BJ printed AlN component corresponds to wurtzite crystal structure showing the principal plane directions at (001), (002) and (101) which is in a complete agreement with those reported by Xiong *et al.*, [9].

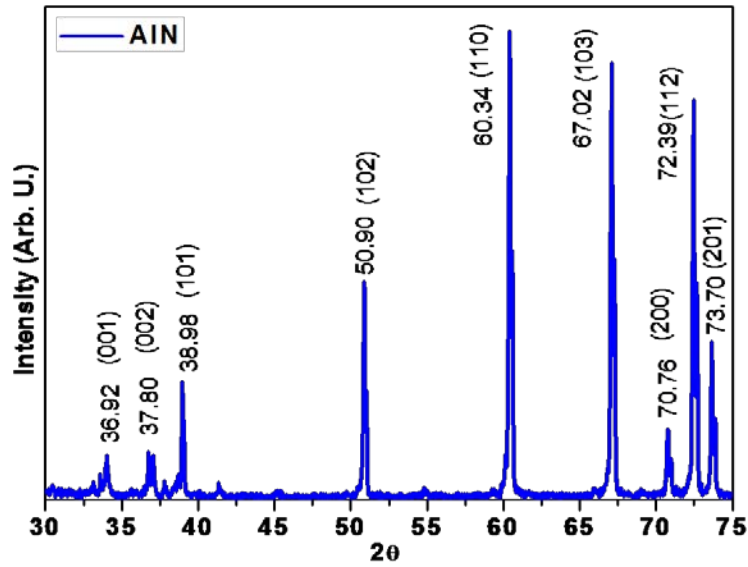


Figure 12. XRD of AlN components after HIPing process.

### 3.4 TC measurements

Here we present the TC properties results measured for an AlN pellet component fabricated by BJ according to the previously discussed dimensions and sintering thermal conditions.

#### 3.4.1 TC at sintering conditions

Figure 13 from a) to c) shows the TC measurements of AlN 3D printed pellet with sintering process from 25 °C to 500 °C, results are presented such as a) specific heat, b) thermal diffusivity, and c) TC, respectively. TC results were found at 2.8 W/m\*K and 1.4 W/m\*K at room temperature and 500 °C, respectively.

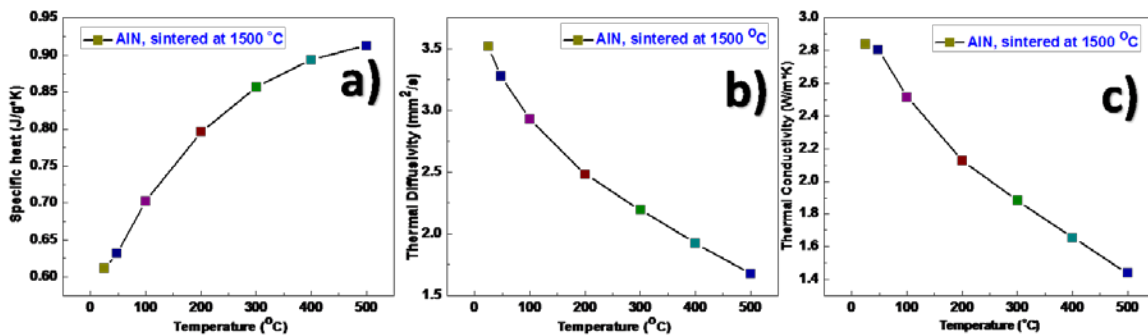


Figure 13. TC measurements of AlN 3D fabricated pellet with sintering process from 25 °C to 500 °C: a) Specific heat (J/gK), b) Thermal diffusivity ( $\text{mm}^2/\text{s}$ ), and c) TC ( $\text{W}/\text{mK}$ ).

### 3.4.2 TC at HIPing conditions

The TC properties results of AlN pellet component with HIPing conditions are presented in figure 14 from a) to b). Fig. 14a) shows a plot showing the specific heat measurements obtained in the temperature range from 25 °C to 500 °C. Figure 14b) shows a plot with the thermal diffusivity values in the same range of temperatures. Figure 14c) shows a plot of TC as a function of the temperature in the range from 25 °C to 500 °C, in the range from 4.82  $\text{W}/\text{m}^*\text{K}$  to 3.17  $\text{W}/\text{m}^*\text{K}$ .

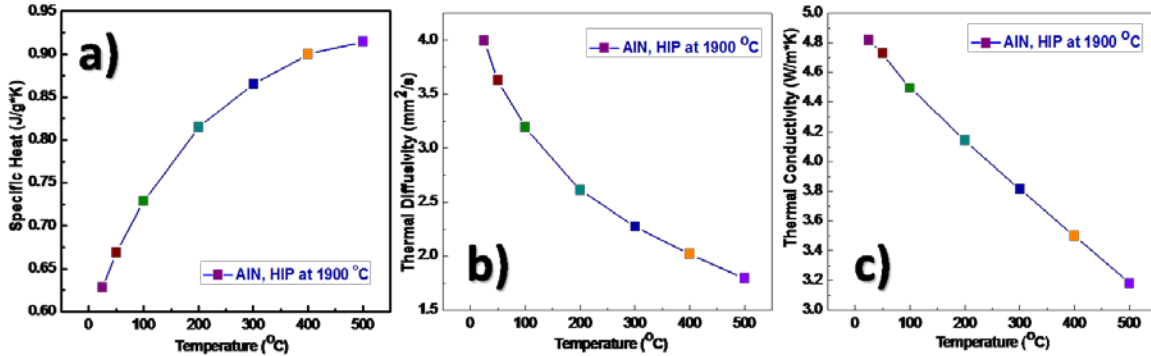


Figure 14. TC measurements of AlN 3D printed pellet with HIPing from 25 °C to 500 °C: a) Specific heat ( $\text{J}/\text{gK}$ ), b) Thermal diffusivity ( $\text{mm}^2/\text{s}$ ), and c) TC ( $\text{W}/\text{mK}$ ).

The TC results obtained are mainly affected by the average size of microcrystals, density, and synthesis method and fabrication process of components [9]. The fabrication method employed here of BJ with HIPing obtained good printed components. Nevertheless, AlN 3D printed components densification through sintering and HIPing may induce some contamination and oxidation. It is well known that oxygen is a typical contamination of AlN, located at the surface of AlN grains as aluminum oxide or oxynitrides [10]. In single crystals of high purity this value can reach  $\sim 320 \text{ W}/(\text{m}^*\text{K})$  at room temperature, but for sintered polycrystals values in the range from 17-285  $\text{W}/(\text{m}^*\text{K})$  are more typical. In general, AlN 3D printing of polycrystalline ceramics exhibit lower thermal conductivities compared with their associated AlN single crystals [11]. As a result of impurities or lattice defects in AlN 3D fabricated components, phonon scattering may occur which leads to a decrease in thermal conductivity. One of the differences between AlN

single crystals, polycrystalline ceramic and AlN 3D fabricated components is that, for polycrystalline materials, the heat carrying process is by mean of phonons which propagate differently in each system network [12]. In single crystals the heat carrying is influenced by their nucleation, stoichiometric chemical homogeneity, mechanical stresses and phase transition in TC ceramics materials.

#### **4. Conclusions**

In this work we have presented results of BJ production of AlN components having high quality thermal conductivity properties for the first time. The structural aspects and thermal conductivity properties were analyzed by using LFM, SEM, EDS and XRD, respectively. The XRD pattern result showed the characteristic crystallographic planes of AlN 3D printed components at (001), (002), and (101) related to wurtzite crystal structure. The SEM results showed that the BJ produced AlN components subjected to HIPing exhibited a crystalline structure due to the formation of well-defined grain boundaries. With LFM, it was found that thermal conductivity properties of HIPed BJ produced AlN in the interval from 25 °C to 500 °C ranged from 4.82 W/m\*K to 3.17 W/m\*K, respectively. In summary, the observed values of the printing parameters, binder density, powder packing rate, binder saturation level, and thermal conductivity properties found in BJ produced AlN components were shown be useful for the development of new devices for use in electronic devices including heat sinks. In future experiments, we propose sintering of BJ AlN at higher temperatures with the prospect of increasing densification. Future work also includes the application of BJ to other technical or engineering ceramics.

#### **Acknowledgments**

Carlos A. Diaz Moreno thanks Mexico's Consejo Nacional de Ciencia y Tecnología (CONACYT) for support through Postdoctoral Abroad Program, Solicitation No. 250381 at The University of Texas at El Paso. Carlos Diaz special thanks to J. Gonzalez for training in the 3D printer M-Lab ExOne technology. Authors thank Kazi Masum, Gil Siqueiros, Lluvia Herrera,

and Dr. Robert Bronson for contributing during research. Finally, authors thank W. M. Keck Center 3D Innovation facilities.

### Conflicts of Interest:

All contributing authors declare no conflict of interest.

### References

- [1] J. A. Gonzalez, J. Mireles, Y. Lin, R.B. Wicker, Characterization of ceramic components fabricated using binder jetting additive manufacturing jetting additive manufacturing technology, *Ceramic International* **42** (2016) 10559-10564.
- [2] Y. Bai, C. B. Williams, An exploration of binder jetting of copper, *Rapid Prototyping Journal*, **21** (2015) 177-185.
- [3] I. Gibson, D. Rosen, B. Stucker, *Additive Manufacturing Technologies*, Second Edition, Springer, 2015, USA.
- [4] M. Hirano, K. Kato, T. Isobe, T. Hirano, Sintering and characterization of fully dense aluminum nitride ceramics, *J. of Mater. Science* **28** (1993) 4725-4730.
- [5] J. H. Harris, Sintered aluminum nitride ceramics for high power electronic applications, *JOM* **50** (1998) 56-60.
- [6] L. Rabinskiy, A. Ripetsky, S. Sitnikov, Y. Solyaev, R. Kahramanov, Fabrication of porous silicon nitride ceramics using binder jetting technology, *IOP Conf. Ser. Mater. Sci. Eng.* **140** (2016) 12023.
- [7] Y. Xiong, H. Wang, Z. Fu, Transient liquid-phase sintering of AlN ceramics with CaF<sub>2</sub> additive, *J. of the Europ. Ceram. Soc.* **33** (2013) 2199-2205.
- [8] W. Du, C. Ma, X. Ren, Z. Pei, Binder Jetting Additive Manufacturing of Ceramics: A Literature Review, *ASME-IMECE* **14** (2017) 1-12, doi:10.1115.
- [9] J. Jarriage, J. P. Lecompte, J. Mullot, G. Müller, Effect of oxygen on the thermal conductivity of aluminum nitride ceramics, *J. of the European Ceramic Society* **17** (1997) 1981-1895.
- [10] C. F. Chen, M. E. Perisse, A. F. Ramirez, P. Padture, H. M. Chan, Effect of grain boundary phase on the thermal conductivity of aluminum nitride ceramics, *J. of Mat. Sci.* **29** (1994) 1595-1600.
- [11] A. Franco Júnior, D. J. Shanafield, Thermal conductivity of polycrystalline aluminum nitride (AlN) ceramics, *Cerâmica* **50** (2004) 247-253.
- [12] L. E. McNeil, M. Grimsditch, R. H. French, Vibrational Spectroscopy of Aluminum Nitride, *J. Am. Ceram. Soc.* **76** (1993) 1132-1136.